Poly(arylene ether ether nitrile)s Containing Flexible Alkylsulfonated Side Chains for Polymer Electrolyte Membranes

Li Sheng,[1] Tomoya Higashihara,[2] Mitsuru Ueda,[3] Teruaki Hayakawa[1]

[1]Department of Organic and Polymeric Materials, Graduate School of Science and Engineering, Tokyo Institute of Technology, 2-12-1 O-okayama, Meguro-ku, Tokyo 152-8552, Japan
[2]Department of Polymer Science and Engineering, Faculty of Engineering, Yamagata University, 4-3-16 Jonan, Yonezawa, Yamagata 992–8510, Japan
[3]Department of Chemistry, Kanagawa University, 3-27-1 Rokkakubashi, Kanagawa-ku, Yokohama 221–8686, Japan
Correspondence to: T. Higashihara (E-mail: thigashihara@yz.yamagata-u.ac.jp) or T. Hayakawa (E-mail: hayakawa.t.ac@m.titech.ac.jp)

Received 2 July 2013; accepted 1 October 2013; published online 18 October 2013
DOI: 10.1002/pola.26971

ABSTRACT: A series of poly(arylene ether ether nitrile)s with different chain lengths of the alkylsulfonates (SPAEEN-*x*: *x* refers number of the methylene units) are successfully synthesized for fuel cell applications. The polymers produced flexible and transparent membranes by solvent casting. The resulting membranes display a high thermal stability, oxidative stability, and higher proton conductivity than that of Nafion 117 at 80 °C and 95% relative humidity (RH). Furthermore, the SPAEEN-12 with the longest alkylsulfonated side chain exhibits a higher proton conductivity at 30% RH than that of SPAEEN-6 despite the lower IEC value, which indicates that the introduction of longer alkylsufonated side chains to the polymer main chain induces an efficient proton conduction by the formation of a well-developed phase-separated morphology. © 2013 Wiley Periodicals, Inc. J. Polym. Sci., Part A: Polym. Chem. **2014**, *52*, 21–29

KEYWORDS: alkylsulfonated side chain; fuel cell; poly(arylene ether ether nitrile); polymer electrolyte membrane; proton conductivity

INTRODUCTION The polymer electrolyte membrane (PEM) is the key component of the PEMFC, because it serves as the separator of the electrodes and transports protons from the anode to the cathode. PEMs that have received the most attention in recent years are fully fluorinated polymers with acid-functionalized side chains, such as Dupont's Nafion® and Dow Chemical's Aquivion®, due to their good proton conductivity, excellent chemical stability and long-term durability. However, they suffer from some drawbacks, such as a high production cost, poor thermomechanical properties above 80 °C, environmental incompatibility and high permeability of the fuels and oxygen. To date, numerous sulfonated aromatic hydrocarbon-based polymers, which contain sulfonic acid groups on the polymer main chain, have been already reported as alternative membranes.[1–15]

The low-cost productivity is an attracting advantage for hydrocarbon-based polymers in comparison to the perfluoropolymers. However, most of them have failed to meet the requirements of a high proton conductivity under a low relative humidity (RH) and durability under fuel cell operating conditions. To improve the proton conductivity at a low RH, increasing the content of the sulfonic acid groups in the polymer main chain, that is, the higher ion exchange capacity (IEC) value, is an effective way. Litt et al.,[16] for example, reported the synthesis of poly(*p*-phenylene disulfonic acid) with the IEC higher than 8.0 mequiv g^{-1}. The proton conductivity value was about 11 times higher than that of Nafion® NR-212 even at 30% RH and 80 °C, which has never yet been reported. However, this membrane absorbed a large amount of water, significantly swelled, and the proton conductivity could not be measured above 65% RH. Therefore, to prepare high performance PEMs for using under fuel cell conditions cannot only focus on increasing the IEC. Recently, the Okamoto and Watanabe groups reported a series of side chain type sulfonated polyimides (SPIs) including both the short side chains (sulfopropoxy and sulfobutoxy groups) and long side chains.[17–22] The resulting membranes showed a higher hydrolytic stability compared to the main chain type SPIs, because the sulfonic acid groups were located on flexible side chains separated from the main chains, which reduced the chances of nucleophilic attack by water on the imide linkage, and also displayed some improvement of proton conductivity by forming a well-dispersed hydrophilic domains compared with the main chain type ones.[2] However, the proton conductivity of SPIs could not be improved even the number of aliphatic carbons were extended to 12,[20,21] probably due to the bulky imide ring in the main chain, which increases the distance between the sulfonic acid groups of the SPI. On the other hand, appropriate high IEC, which is required for high proton transport, is difficult to obtain for increasing the length of side chain on SPIs.[20] Zhang group also reported side chain type polymers for PEMs,[23] they chose poly(arylene ether sulfone)s with the cardo structure as the main chain and introduced long side chains with the number of alkyl carbon of 10. However, the proton conductivity was lower than that of Nafion even in water due to low density of the alkylsulfonic acid groups in the polymers.

In this study, the aromatic poly(arylene ether ether nitrile)s (SPAEEN-*x*) with high density of the alkylsulfonic acid groups were successfully prepared. The nitrile groups were introduced into the polymer main chain to suppress the water uptake according to the previous report.[24] Furthermore, the effect of chain lengths of alkylsulfonic acid groups on the membrane properties, such as thermal stability, oxidative stability, mechanical strength, water uptake, and proton conductivity was investigated. We found that the membrane SAPEEN-12 with the lower IEC value of 1.89 mequiv g^{-1} showed higher proton conductivity than the membrane SPAEEN-6 with the higher IEC value of 2.32 mequiv g^{-1} at low RH by the formation of well-developed nanophase-separated morphology, which was supported by atomic force microscope (AFM) images.

EXPERIMENTAL

Materials

5-Methoxyresorcinol (MRS) was purchased from Aldrich. 2,6-Difluorobenzonitrile (DFBN), methoxyhydroquinone (MHQ), boron tribromide (17% in dichloromethane, ca. 1 mol L^{-1}), 1,1,2,2-tetrachloroethane, 1,3-propanesultone, 1,4-butanesultone, 1,6-dibromohexane, 1,10-dibromodecane, and 1,12-dibromododecane were purchased from TCI. 1,1,2,2-Tetrachloroethane was distilled under reduced pressure from finely ground $CaCl_2$. The other reagents were used as received.

Synthesis of Sodium 6-Bromohexylsulfonate, Sodium 10-Bromodecylsulfonate, and Sodium 12-Bromododecylsulfonate

Sodium 6-bromohexylsulfonate, sodium 10-bromodecylsulfonate, and sodium 12-bromododecylsulfonate were synthesized following the procedure described in a report.[25] A typical example for the synthesis of sodium 6-bromohexylsulfonate is as follows:

To a 50 mL flask with a reflux condenser and a nitrogen inlet were added 1,6-dibromohexane (4.88 g, 20.0 mmol), ethanol (10.0 mL), and deionized water (4.00 mL). The mixture was heated to boiling temperature, and a solution of sodium sulfite (0.756 g, 6.00 mmol) in deionized water (2.70 mL) was added dropwise, after refluxing for 2 h, most of solvent was removed by evaporation. The remaining mixture was washed with acetone. Then the solid product was extracted from the sodium bromide and unconverted sodium sulfite with boiling 95% ethanol, thoroughly washed with acetone and then dried at 110 °C for 24 h in vacuum.

Yield: 77%. ^1H NMR (300 MHz, DMSO-d_6, δ): 1.21–1.46 (4H, $—CH_2—CH_2—$), 1.50–1.65 (2H, $—CH_2—CH_2SO_3Na$), 1.72–1.86 (2H, $BrCH_2—CH_2—$), 2.37–2.46 (2H, $—CH_2—SO_3Na$), 3.47–3.56 (2H, $Br—CH_2—$).

Synthesis of Poly(arylene ether ether nitrile) Containing Methoxy Groups (MPAEEN)

The MPAEEN was synthesized by nucleophilic substitution reaction. DFBN (1.67 g, 12.0 mmol), MHQ (1.26 g, 9.00 mmol), MRS (0.420 g, 3.00 mmol), K_2CO_3 (2.00 g, 14.4 mmol), DMAc (15.0 mL), and toluene (15.0 mL) were added into a dry 100 mL three-neck flask equipped with a nitrogen inlet and a Dean-Stark trap. The reaction mixture was heated to 140 °C for 3 h. After dehydration and removal of toluene, the reaction temperature was increased to 160 °C. When the solution viscosity had apparently increased, the mixture was cooled to 120 °C, then was slowly poured into a large excess of deionized water. The fiber-like precipitate was filtered off, washed with deionized water. The polymer was reprecipitated from 2 wt % DMAc solution into ethanol, and dried in vacuum at 100 °C for 24 h.

Yield: 98%. FTIR (membrane): ν2943–2835 (C—H), 2230 (C≡N), 1602 (C═C), 1192, 1240 (Ar—O—Ar), 1130 cm^{-1} (O—C).

Synthesis of Poly(arylene ether ether nitrile) Containing Hydroxyl Groups (HPAEEN)

Demethylation reaction was described as follow: MPAEEN (3.20 g) was dissolved into 200 mL anhydrous 1,1,2,2-tetrachloroethane in a 500 mL three-neck flask with a nitrogen inlet. The solution was cooled down to 0 °C (ice bath) and 1 M solution of BBr_3 in CH_2Cl_2 was added dropwise. After 12 h, the resulting polymer was filtered, washed with ethanol and deionized water several times, and then dried under vacuum at 100 °C for 24 h.

Yield: 97%. FTIR (membrane): ν3525–3260 (—OH), 2230 (C≡N), 1602 (C═C), 1192, 1240 cm^{-1} (Ar—O—Ar).

Synthesis of Poly(arylene ether ether nitrile) with Pendant Alkylsufonic Acid Groups (SPAEEN-x)

A typical synthetic procedure for SPAEEN-6 is described as follows: HPAEEN (0.450 g, 2.00 mmol) was added into a 50 mL dry two-necked flask equipped with a Dean-Stark trap, a condenser and a nitrogen inlet. Anhydrous DMSO (8.00 mL) was then added via a syringe through a septum cap. After HPAEEN was completely dissolved in DMSO at 100 °C, NaOH (0.160 g, 4.00 mmol), and cyclohexane (8.00 mL) were added. The mixture was heated at 100 °C for 2 h to remove water. After removal of cyclohexane and water, sodium 6-bromo-hexylsulfonate (1.07 g, 4.00 mmol) and a suitable quantity of potassium iodide (KI) were added into the mixture. Then the reaction was kept at 100 °C for 24 h. The

$$\mathrm{Br}\left(\mathrm{CH_2}\right)_n\mathrm{Br} + \mathrm{Na_2SO_3} \xrightarrow{\mathrm{EtOH/H_2O}} \mathrm{Br}\left(\mathrm{CH_2}\right)_n\mathrm{SO_3Na} \qquad (n = 6, 10, 12)$$

SCHEME 1 Synthesis of sodium bromoalkylsulfonates.

resulting polymer was obtained by carefully pouring the solution into water, filtered, washed thoroughly with water, ethanol and dried under vacuum at 80 °C for 10 h.

Yield: 95%. FTIR (membrane): ν2230 (C≡N), 1602 (C=C), 1192, 1240 (Ar—O—Ar), 1128, 1047 (O=S=O).

Membrane Formation and Proton Exchange

Membranes were prepared by casting the SPAEEN-*x* (in their sodium form) solution in DMSO onto glass plates and dried at 80 °C for 24 h. Proton exchange was performed by immersing the membranes in 2.0 M H_2SO_4 at 40 °C for 3 days. The proton exchanged membranes were washed with deionized water for 1 day.

Measurements

^{1}H NMR spectrum was recorded on a JEOL JNM-AL 300 NMR spectrometer using DMSO-d_6 as solvent and tetramethylsilane (TMS) as an internal standard. Number- and weight-average molecular weights (M_n and M_w) were measured by gel permeation chromatography (GPC) on a Viscotek TDA 302 system with a TSK-GEL a-M column and *N,N*-dimethylformamide (DMF) as eluent. Thermogravimetric analysis (TGA) was performed on a TA Instruments TG/DTA 7300 in nitrogen. Prior to measurement, all the samples were preheated at 150 °C for 30 min to remove any absorbed moisture. Subsequently the samples were cooled to 50 °C and then heated to 550 °C at a heating rate of 10 °C min^{-1}. Ion exchange capacity (IEC) was measured by a titration method. The samples were immersed in saturated NaCl solution at room temperature for 3 days. After that, the NaCl solution was directly titrated with 0.02 M NaOH using phenolphthalein as pH indicator. Tensile measurements were performed with a universal testing instrument (AGS-X 349–05489A, Shimadzu, Japan) at 20 °C and around 50% RH at a crosshead speed of 2 mm/min. The oxidation stability of the membranes was determined by Fenton's test. The samples were soaked in the Fenton's reagent (3% H_2O_2 containing 20 ppm $FeSO_4$) at room temperature. The disappearance time of the samples was used to evaluate the radical oxidation stability of the membrane. Water uptake of the membrane was measured by placing the membrane in a thermocontrolled humidity chamber. The membranes were set at desired values and kept constant for 2 h at each point. Then the membrane was taken out, and quickly weighed on a microbalance. Water uptake (WU) was calculated according to the following equation:

$$\mathrm{WU} = (W_s - W_d)/W_d \times 100\ \mathrm{wt\%} \tag{1}$$

where W_s and W_d are the weights of wet and dried membranes, respectively. Water sorption was also expressed as the average number of water molecules per ion exchange site ($[H_2O]/[SO_3^-]$), often referred to as λ value, and calculated according to the following equation:

$$\lambda = [H_2O]/[SO_3^-] = \mathrm{WU}\ (\%) \times 10/[18 \times \mathrm{IEC}\ (\mathrm{mmol\ g^{-1}})] \tag{2}$$

Dimensional change of a hydrated membrane was also investigated by placing the membrane in a thermocontrolled humid chamber (80 °C) at desired RH for 2 h, the changes of length and thickness were calculated from the equation:

$$\Delta l = (l_s - l_d)/l_d \times 100\% \tag{3}$$

$$\Delta t = (t_s - t_d)/t_d \times 100\% \tag{4}$$

where l_s and t_s are the length and thickness of the wet membrane, respectively, l_d and t_d refer to those of the dried membrane. Proton conductivity was measured using a two-probe electrochemical impedance spectroscopy technique over the frequency from 5 Hz to 1 MHz (Hioki 3532-80). The samples were 8-mm long, 8-mm wide, and 68- to 109-μm thick. Proton conductivity (σ) was calculated from the following equation:

$$\sigma = d/(t_s w_s R) \tag{5}$$

where d is the distance between the two electrodes, t_s and w_s are the thickness and width of the membrane, and R is the measured resistance. Tapping mode atomic force microscope (AFM) images were taken by using Seiko Instruments SPA-400 with a stiff cantilever of Seiko Instruments DF-20.

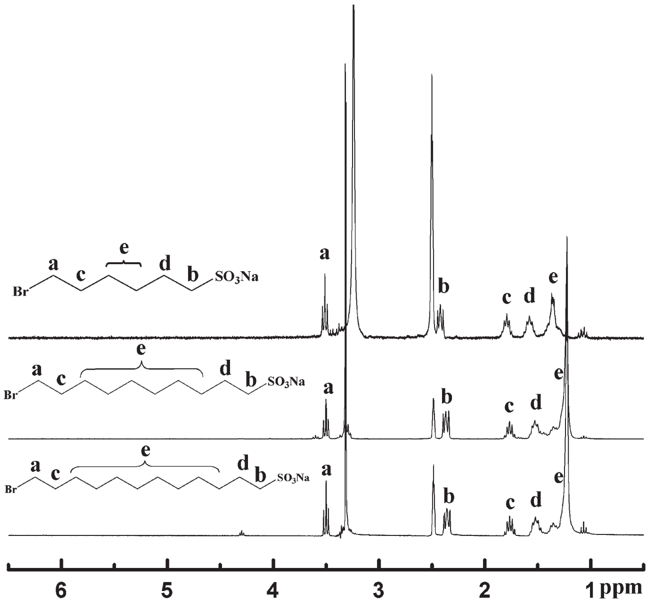

FIGURE 1 ^{1}H NMR spectra of sodium bromoalkylsulfonates.

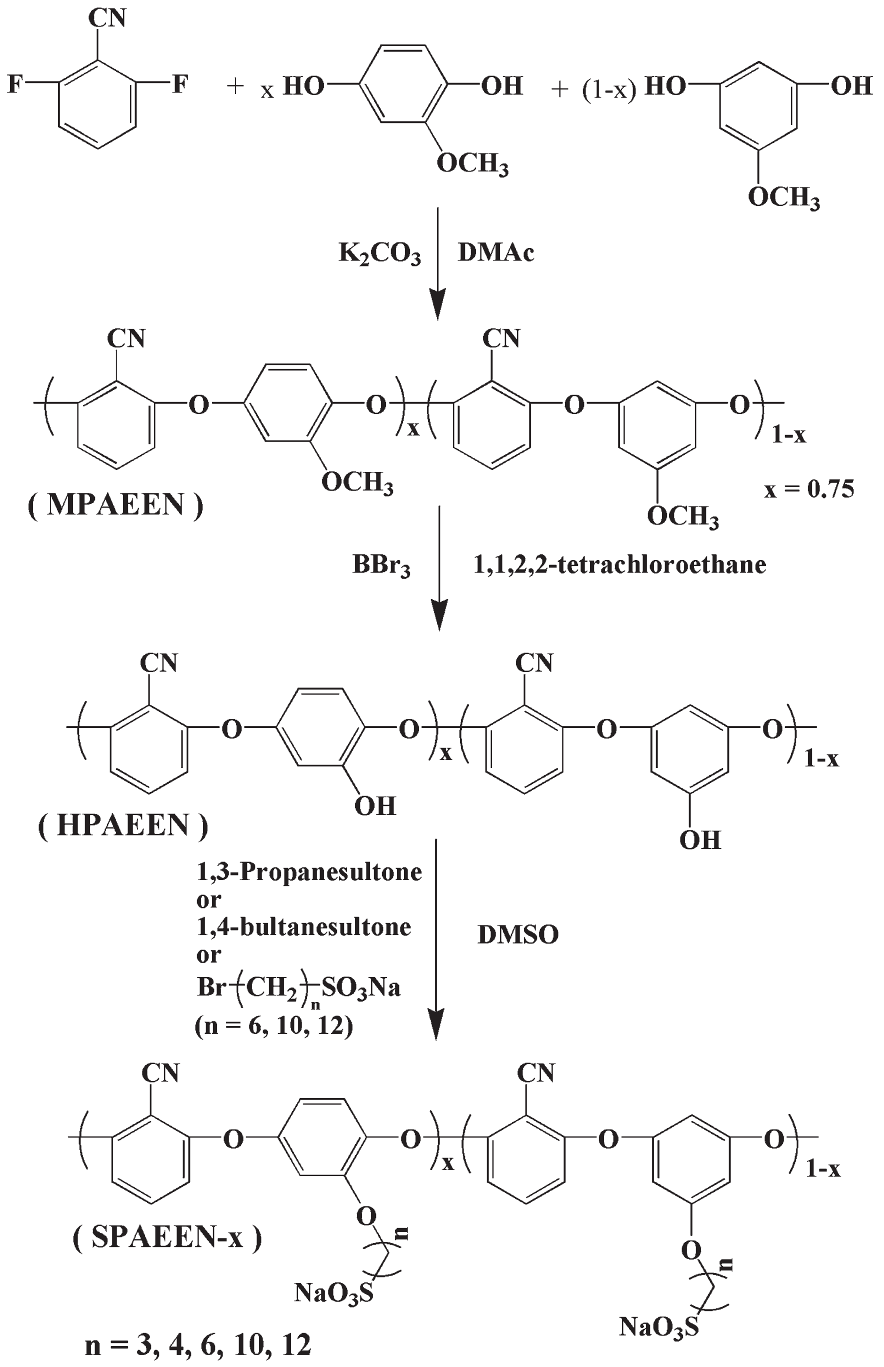

SCHEME 2 Synthesis of poly(arylene ether ether nitrile)s with pendant alkylsufonic acid groups (SPAEEN-*x*).

RESULTS AND DISCUSSION

Synthesis of Sodium Bromoalkylsulfonates and Polymers

As shown in Scheme 1, various sodium bromoalkylsulfonates were prepared according to the previous paper.[25] The chemical structures of sodium 6-bromohexylsulfonate, sodium 10-bromodecylsulfonate, and sodium 12-bromododecylsulfonate were confirmed by ^{1}H NMR spectroscopy (Fig. 1). New peaks at 2.36–2.46 ppm corresponding to the methylene protons next to the —SO_3Na groups are clearly observed. All the other peaks are also well assigned to the corresponding structures. Poly(arylene ether ether nitrile)s with pendant alkylsufonic acid groups (SPAEEN-*x*, *x* refers the number of methylene units) were prepared via a three-step reaction as shown in Scheme 2. First, the polycondensation of DFBN with MRS was conducted at 160 °C, leading to a low molecular weight polymer because of premature precipitation of the polymer. Then, MHQ in the place of MRS was employed to improve the solubility of the resulting polymer. Although the high molecular weight polymer could be easily prepared

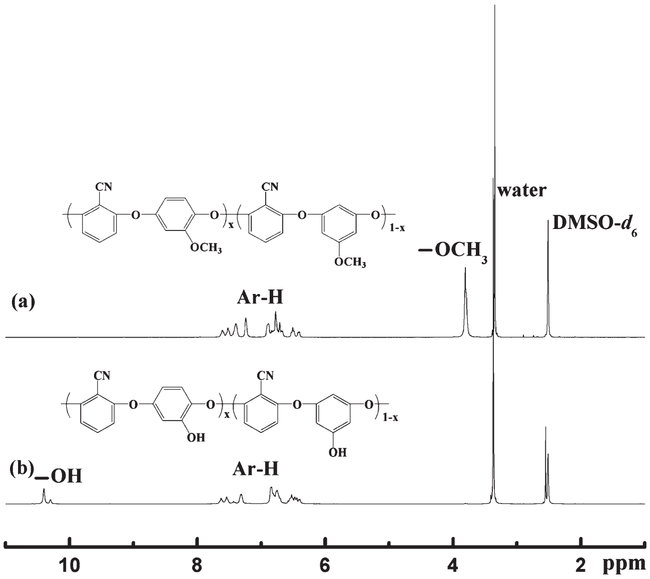

FIGURE 2 ^{1}H NMR spectra of (a) MPAEEN and (b) HPAEEN.

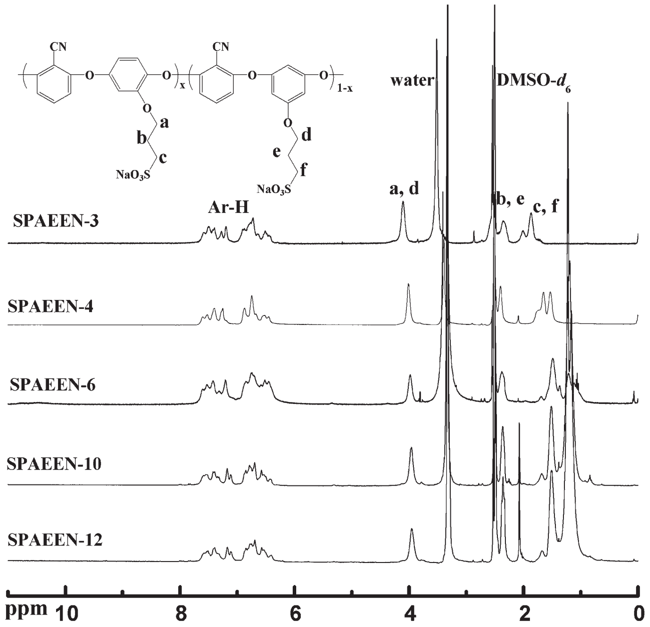

FIGURE 4 ^{1}H NMR spectra of SPAEEN-*x*.

from DFBN and MHQ, the resulting polymer showed a limited solubility in halogenated hydrocarbons which are suitable solvents for the demethylation of methoxy groups using BBr_3. Finally, MPAEEN ($M_n = 41{,}000$, $M_w = 116{,}000$) was prepared by the nucleophilic substitution polycondensation of DFBN with MHQ and MRS in DMAc at 160 °C.

The demethylation of the methoxy groups was conducted using BBr_3 in 1,1,2,2-tetrachloroethane. HPAEEN was precipitated during the reaction due to the polar nature of the phenol groups. Figure 2 shows the ^{1}H NMR spectra of MPAEEN and HPAEEN. The characteristic methoxy protons at 3.79 ppm in the initial MPAEEN disappear in the HPAEEN, and the peak around 10.35 ppm corresponding to the phenol proton appears, indicating that the deprotection had successfully proceeded. Finally, SPAEEN-*x* was obtained by the reaction of the alkanesultones or sodium bromoalkylsulfonates with HPAEEN in the presence of NaOH. Before adding the alkanesultones or sodium bromoalkylsulfonates, the water in the reaction mixture was removed by azeotropic distillation with cyclohexane. The structures of the SPAEEN-*x* were also confirmed by the FTIR and ^{1}H NMR spectroscopy. The FTIR spectra of the SPAEEN-*x* in their sodium form are shown in Figure 3. The SPAEEN-*x* show characteristic bands at 1047 and 1128 cm^{-1} assigned to the O=S=O stretching vibration of the sulfonate groups. The band at 2230 cm^{-1} corresponding to the stretching vibrations of the nitrile group was also observed. The ^{1}H NMR spectra of SPAEEN-*x* are shown in Figure 4, exhibiting characteristic methylene protons next to

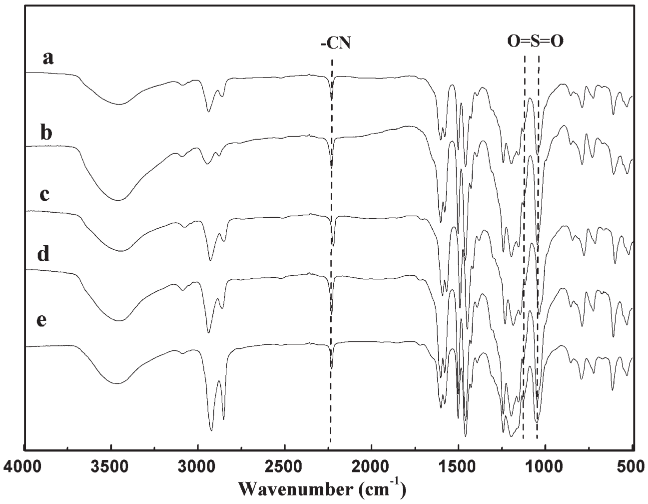

FIGURE 3 FTIR spectra of SPAEEN-*x* in sodium form [(a) SPAEEN-3; (b) SPAEEN-4; (c) SPAEEN-6; (d) SPAEEN-10; (e) SPAEEN-12].

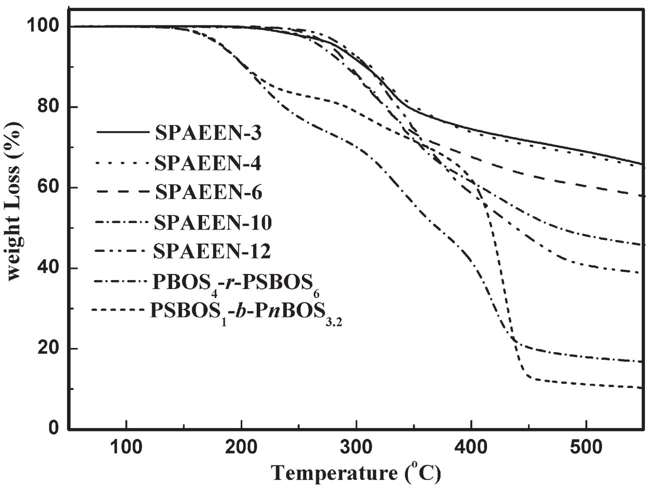

FIGURE 5 TGA curves of the SPAEEN-*x* membranes, crosslinked sulfonated random ($PBOS_4$-*r*-$PSBOS_6$)[26] and block copolystyrene derivatives ($PSBOS_1$-*b*-P*n*$BOS_{3.2}$)[27] in acid form under N_2.

TABLE 1 Thermal, Mechanical Properties, and Oxidative Stability of SPAEEN-*x* Membranes

					Oxidative Stability	
Samples	$T_{d\ 5\%}$ (°C)	Maximum Stress (MPa)[a]	Young's Modulus (MPa)[a]	Elongation at Break (%)[a]	τ (h)[b]	RW (wt %)[c]
SPAEEN-3	285	–[d]	–	–	43	0
SPAEEN-4	284	19	714	25	44	0
SPAEEN-6	278	22	522	15	62	68
SPAEEN-10	270	18	435	25	>80	>95
SPAEEN-12	289	–	–	–	>80	>95

[a] Measured at 20 °C under 50% RH.

[b] τ(h): Disappearance time: measured by soaking the membranes in Fenton's reagent (3% H_2O_2 containing 20 ppm $FeSO_4$) at room temperature.

[c] RW (wt %): Remaining weight: measured by soaking the membranes in Fenton's reagent (3% H_2O_2 containing 2 ppm $FeSO_4$) at 80 °C for 1 h.

[d] Has not measured.

the sodium sulfonate group at 2.37 ppm, while no hydroxyl protons were observed.

Thermal Properties

The thermal stability of the polymer SPAEEN-*x* in the acid forms was investigated by TGA analysis under nitrogen (Fig. 5). All the samples were preheated at 150 °C for 30 min in the TGA furnace to remove any moisture. For comparison, the crosslinked sulfonated random ($PBOS_4$-*r*-$PSBOS_6$)[26] and block copolystyrene derivatives ($PSBOS_1$-*b*-P*n*$BOS_{3.2}$)[27] having flexible alkylsulfonated side chains and hydrophobic alkoxy chains are also shown in Figure 5. All the SPAEEN-*x* membranes showed a two-stage weight loss behavior. The first stage weight loss temperature that started from 220 °C is possibly associated with the loss of bound water and degradation of the sulfonic acid groups, which is much higher than that of the $PBOS_4$-*r*-$PSBOS_6$ (150 °C)[26] and $PSBOS_1$-*b*-P*n*$BOS_{3.2}$ (150 °C).[27] The second stage weight loss temperature at around 350 °C is likely related to the degradation of the alkyl side chain and polymer main chain. The 5 wt % weight loss temperatures ($T_{d5\%}$) of all the SPAEEN membranes summarized in Table 1 are higher than 270 °C. The TGA results indicate that the SPAEEN-*x* have high thermal stability, which is high enough for the applications in medium temperature (100–180 °C) fuel cells.

IEC, Water Uptake, and Dimensional Change

The IEC values were determined by a titration method, and the measured IEC values of the SPAEEN-*x* membranes are in the range of 1.89–2.69 mequiv g^{-1} (Table 2). The water uptake (WU) and swelling ratio of the PEMs are very important properties that are significantly related to the proton conductivity and mechanical strength. Moreover, the IEC values of the sulfonated aromatic polymers generally dominate the WU. The WU and hydration number (λ) of SPAEEN-3 are the highest among the studied membranes due to its high IEC (Fig. 6). However, the WU of SPAEEN-3 at 80 °C under 95% RH is lower than 60%, which corresponds to the absorption of <12 water molecules per a sulfonic acid group. One plausible explanation is the presence of nitrile-nitrile dipole interactions that combine to limit the WU, which has been reported by Pivovar group.[24] In addition, the interaction between the nitrile and sulfonic acid groups may be important as nitrile groups have been found to associate with sulfonic acid groups through bridging water molecules in specific spectroscopic studies.[24,28] On the other hand, the WU and λ dramatically decrease at 95% RH when the length of the alkyl side chains is increased. The SPAEEN-3 membrane, for example, has a WU around 57%, which is two times higher than that of the SPAEEN-12 membrane (25%). The dimensional change in all the SPAEEN-*x* membranes was

TABLE 2 Ion Exchange Capacities (IEC), Water Uptake (WU), and Proton Conductivity (σ) of the SPAEEN-*x* Membranes

	IEC (mequiv g^{-1})		WU[a] (wt %)		σ[a] (*m*S/cm)	
Samples	Theoretical	Measured[b]	30% RH	95% RH	30% RH	95% RH
SPAEEN-3	2.87	2.69	5.65	57.3	1.71	212
SPAEEN-4	2.76	2.61	5.37	53.5	1.06	226
SPAEEN-6	2.57	2.32	4.67	35.6	0.416	175
SPAEEN-10	2.24	1.99	2.31	26.7	0.750	150
SPAEEN-12	2.11	1.89	2.89	25.0	0.877	137

[a] Measured at 80 °C.

[b] By titration method.

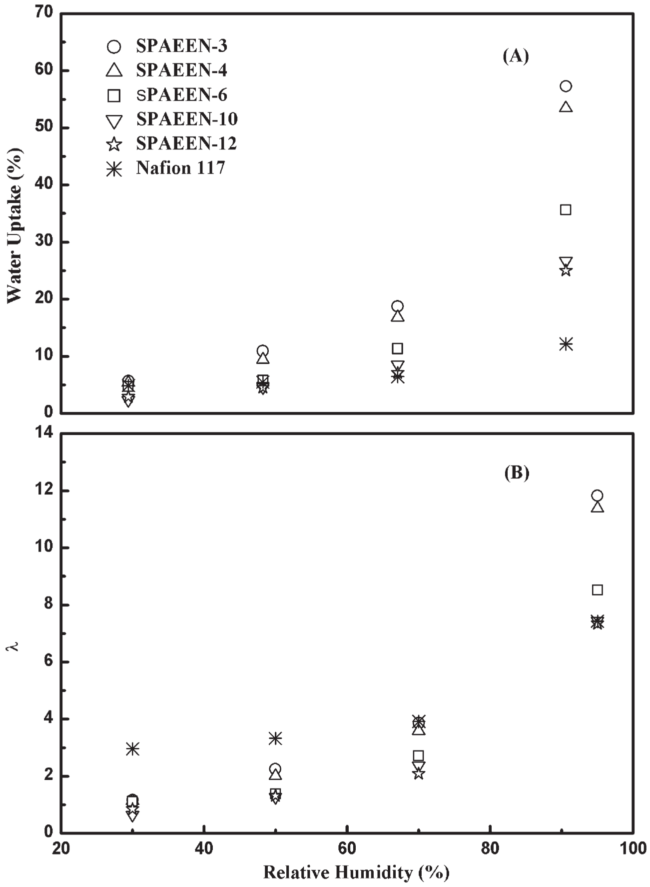

FIGURE 6 Water uptake (A) and hydration number (λ) (B) of SPAEEN-*x* and Nafion 117 under different RH at 80 °C.

also measured at different RHs (50–95%) and 80 °C (Fig. 7). The SPAEEN-*x* membranes show an anisotropic swelling behavior with a slightly higher change in the thickness direction. The SPAEEN-3 membrane with the highest IEC among these membranes displays a dimensional change lower than 13% even at 95% RH. This result indicates that the introduction of the —CN group and long alkylsulfonated side chains can effectively suppress the swelling ratio of the membranes.

Oxidative Stability and Mechanical Properties

It is well known that the poor oxidative stability of the membranes may cause failure during long-term fuel cell operations. Fenton's test is a common method, which has been widely used for evaluation the oxidative stability. The membranes are generally immersed in 3% H_2O_2 containing 20 ppm $FeSO_4$ at room temperature or 3% H_2O_2 containing 2 ppm $FeSO_4$ at elevated temperature (e.g., 80 °C), and the oxidative stability is characterized either by the disappearance time of the membranes or by the weight loss of the membranes as a function of time. In this study, the oxidative stability of all the prepared membranes was evaluated by immersing the samples in Fenton's reagent (3% H_2O_2 aq., 20 ppm $FeSO_4$) at room temperature. The resistance to oxidation of the membranes was measured by observing their dissolution behavior, and these results are summarized in Table 1. The SPAEEN-3 membrane with the highest IEC value resists dissolution in Fenton's reagent for more than 40 h. On the other hand, the membranes with longer alkylsulfonated side chains show better oxidative stability than those with the shorter side chains. The SPAEEN-12 membrane, for example, does not disappear for up to 80 h. Furthermore, the remaining weight of SPAEEN-10 and SPAEEN-12 after soaking in Fenton's reagent (3% H_2O_2 aq., 2 ppm $FeSO_4$) at 80 °C for 1 h, is still greater than 95 wt %, which indicates that the introduction of flexible alkylsufonic acids side chains can improve the oxidative stability. Because the sulfonic acid group is an electro-withdrawing group, when it is directly attached to the aromatic ring of the polymer main chain, it can reduce the electron density of the neighboring aromatic groups by a resonance effect and facilitate the nucleophilic displacement reaction. It would be reasonable to assume that the oxidative degradation of the sulfonated poly(arylene ether)s commences at the *o*-carbons to the ether linkages by attack of the hydroxyl radicals. For the side chain type polymers, the longer alkyl side chains could more effectively separate the polymer main chain from the sulfonic acid groups to keep the main chain in a hydrophobic atmosphere that prevents or reduces the chance of radical attack, and the introduction of the —CN group, which decreases the water

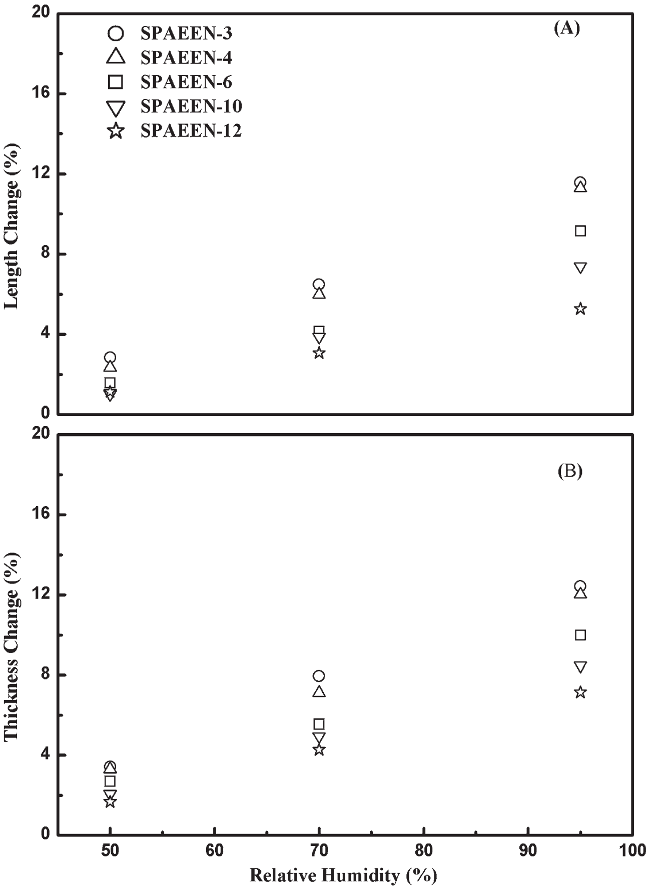

FIGURE 7 Dimensional change of SPAEEN-*x*: length change (A) and thickness change (B) under different RH at 80 °C.

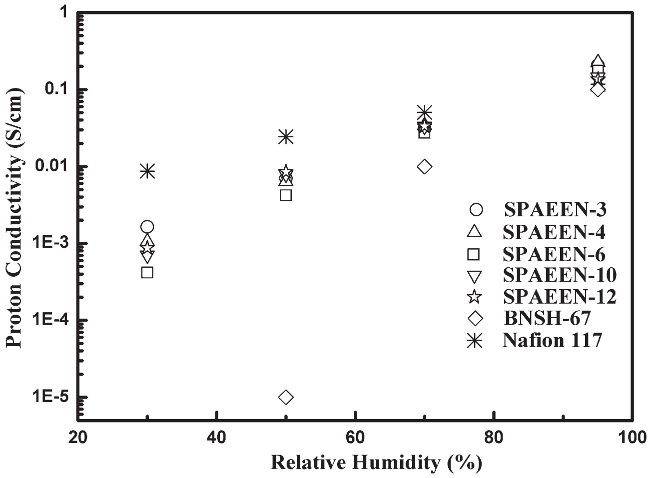

FIGURE 8 Variation of proton conductivity of the SPAEEN-*x*, BNSH-67,[10] and Nafion 117 as a function of RH and 80 °C.

uptake and swelling ratio, could also retard the entrance of the oxidative agent into the membrane.[23]

The tensile properties of the SPAEEN-*x* membranes were measured and the results are listed in Table 1. It can be seen that these membranes (except SPAEEN-3 and SPAEEN-12) show maximum stress in the range of 18–22 MPa, which is similar to that of the crosslinked sulfonated polystyrene with flexible alkylsulfonated side chains,[26,27] while the Young's modulus of the SPAEEN-*x* membranes are much higher than those of the latter due to the high chain rigidity of aromatic polymer backbone.

Proton Conductivity

The proton conductivities of the SPAEEN-*x* membranes were measured at 80 °C under different RH (30–95%) conditions and the results are shown in Figure 8 and compared to that of the Nafion 117 membrane. It can be seen that for all the SPAEEN-*x* membranes, the proton conductivities increase with the increasing RH. They show higher proton conductivities (0.137–0.212 S/cm) than that of Nafion 117 (0.118 S/cm) at 95% RH. It is well known that the proton conductivity of the sulfonated aromatic hydrocarbon-based polymers is mainly dependent on the IEC values, and the higher IEC, the higher proton conductivity. The morphology of the membrane is another factor which also affects the proton conductivity. The longer flexible side chains are supposed to favor a well-developed phase separation, which is expected to contribute to the high proton conductivity. In this study, the side chain type SPAEEN-*x* exhibit a higher proton conductivity than that of the other sulfonated poly(ether sulfone)s (BNSH-67),[10] which contain sulfonic acid groups on the main chain. For example, the proton conductivity of the SPAEEN-10 ($\text{IEC} = 1.99$ mequiv g^{-1}) was 8.0×10^{-3} S cm^{-1}, which was higher than that of the BNSH-67 ($\text{IEC} = 2.18$ mequiv g^{-1}) (10^{-5} S cm^{-1}) at 80 °C and 50% RH. The hydrophilic sulfonic acid groups are directly attached to the main chains of BNSH-67, which could reduce the hydrophobicity of the main chain, resulting in poor phase separation. Compared with other side chain type polymers, the conductivity of SPAEEN-12 is much higher than that of sulfonated polyimide with long side chain 12(12)[20] due to the high density of the alkylsulfonic acids. All these results indicate that introduction of flexible side chains and increasing the density of the alkylsulfonic acids in the polymer could effectively improve the proton conductivity.

As described above, the proton conductivity of the sulfonated aromatic hydrocarbon-based polymers is mainly dependent on the IEC values. However, in this study, the SPAEEN-6, SPAEEN-10, and SPAEEN-12 containing an alkyl carbon more than 4 display an interesting phenomenon, their proton conductivities are independent on the IEC values at 30% RH (Table 2). Generally, the decrease of RH would cause the disconnection of SO_3^- clusters and the proton transportation by water molecular motion between clusters becomes dominant for the membranes motion between clusters becomes dominant for the membranes,[29] therefore, the conductivity of these membranes mainly depends on water uptake, which is affected by IEC. For the membranes which maintain the connectivity of ion channel even at low RH, the protons transported easily through the channel. The SPAEEN-12

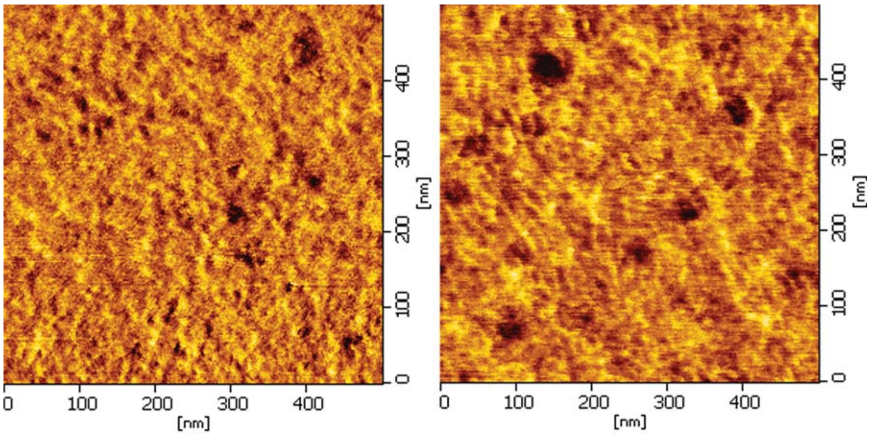

FIGURE 9 AFM image of SPAEEN-6 membrane (L) and SPAEEN-12 membrane (R).

membrane contains the longest flexible aliphatic side chain, which is expected to form ion channel for transporting protons.

Morphology

The microstructure of the SPAEEN-*x* membranes was investigated by AFM. As shown in Figure 9, both SPAEEN-6 and SPAEEN-12 membranes display the formation of phase-separated structures, in which the alkylated sulfonic acids would aggregate into hydrophilic clusters. In the AFM images, more organized phase-separated morphology can be observed for the SPAEEN-12 membrane than that of SPAEEN-6. This indicates that the longer alkyl side chain could induce the formation of well-organized nanodomains. The formation of the domains in a series of SPAEEN membranes would be to improve proton conductivity and oxidative stability. The aggregation of the sulfonic acids supported by longer flexible alkyl chains generates the well-developed nanochannel liked morphology, which could improve the proton conduction at low RH and also prevent from oxidizing the polymer main chain by hydroxyl radical attack.

CONCLUSIONS

A series of SPAEEN-*x* copolymers containing different chain lengths of alkylsulfonates have been prepared by a three-step reaction, that is, polycondensation of DFBN containing a strongly polar —CN group with MRS and MHQ, followed by demethylation and the reaction with alkanesultones or sodium bromoalkylsulfonates. The resulting membranes exhibited a high thermal stability despite the full aliphatic side chains, high oxidative stability against Fenton's reagent at room temperature, low water uptake and dimensional change even at 95% RH. The SPAEEN-3 membrane with the IEC of 2.69 mequiv g^{-1} displayed the highest proton conductivity among these prepared membranes over the entire range of RH from 30 to 95%. On the other hand, the SPAEEN-12 membrane with the longer side chain displayed a lower water uptake and higher proton conductivity (at 30% RH) than those with the shorter side chain membrane SPAEEN-6 in spite of its lower IEC value. The introduction of more than six aliphatic carbons as the side chain may improve the proton conductivity especially at a low RH by forming a well-developed phase separation.

ACKNOWLEDGMENTS

This work was supported by Industrial Technology Research Grant Program in 2011 (#11B02008c) from New Energy and Industrial Technology Development Organization (NEDO) of Japan.

REFERENCES AND NOTES

1 J. Roziere, D. J. Jones, *Annu. Rev. Mater. Res.* **2003**, *33*, 503–555.

2 N. Asano, M. Aoki, S. Suzuki, K. Miyatake, H. Uchida, M. Watanabe, *J. Am. Chem. Soc.* **2006**, *128*, 1762–1769.

3 S. Besse, P. Capron, G. Gebel, F. Jousse, D. Marsacq, M. Pineri, C. Marestin, R. Mercier, *J. New Mater Electrochem Systems* **2002**, *5*, 109–112.

4 C. Genies, R. Mercier, B. Sillion, N. Cornet, G. Gebel, M. Pineri, *Polymer* **2001**, *42*, 359–373.

5 T. Higashihara, K. Matsumoto, M. Ueda, *Polymer* **2009**, *50*, 5341–5357.

6 J. M. Bae, I. Honma, M. Merata, T. Yamamoto, M. Rikukawa, N. Ogata, *Solid State Ionics*, **2002**, *147*, 189–194.

7 J. A. Kerres, *J. Membr. Sci.* **2001**, *185*, 3–27.

8 V. Mehta, J. S. Cooper, *J. Power Sources* **2003**, *114*, 32–53.

9 K. Nakabayashi, K. Matsumoto, M. Ueda, *J. Polym. Sci., Part A: Polym. Chem.* **2008**, *46*, 3947–3957.

10 K. Matsumoto, T. Nakagawa, T. Higashihara, M. Ueda, *J. Polym. Sci., Part A: Polym. Chem.* ,*47*, 5827–5834.

11 K. Nakabayashi, T. Higashihara, M. Ueda, *J. Polym. Sci., Part A: Polym. Chem.* **2010**, *48*, 2757–2764.

12 K. Nakabayashi, T. Higashihara, M. Ueda, *Macromolecules* **2010**, *43*, 5756–5761.

13 X. Guo, J. Fang, T. Watari, K. Tanaka, H. Kita, K. Okamoto, *Macromolecules* **2002**, *35*, 6707–6713.

14 J. Fang, X. Guo, S. Harada, T. Watari, K. Tanaka, H. Kita, K. Okamoto, *Macromolecules* **2002**, *35*, 9022–9028.

15 Y. Yin, J. Fang, H. Kita, K. Okamoto, *Chem. Lett.* **2003**, *32*, 328–329.

16 K. Si, D. Dong, R. Wycisk, M. Litt, *J. Mater. Chem.* **2012**, *22*, 20907–20917.

17 Y. Yin, Y. Suto, T. Sakabe, S. Chen, S. Hayashi, T. Mishima, O. Yamada, K. Tanaka, H. Kita, K. Okamoto, *Macromolecules* **2006**, *39*, 1189–1198.

18 Z. Hu, Y. Yin, K. Okamoto, Y. Moriyama, A. Morikawa, *J. Membr. Sci.* **2009**, *329*, 146–152.

19 Y. Yin, Q. Du, Y. Qin, Y. Zhou, K. Okamoto, *J. Membr. Sci.* **2011**, *367*, 211–219.

20 T. Yasuda, Y. Li, K. Miyatake, M. Hirai, M. Nanasawa, M. Watanabe, *J. Polym. Sci., Part A: Polym. Chem.* **2006**, *44*, 3995–4005.

21 K. Miyatake, T. Yasuda, M. Hirai, M. Nanasawa, M. Watanabe, *J. Polym. Sci., Part A: Polym. Chem.* **2007**, *45*, 157–163.

22 A. Kabasawa, J. Saito, H. Yano, K. Miyatake, H. Uchida, M. Watanabe, *Electrochem. Acta* **2009**, *54*, 1076–1082.

23 N. Gao, F. Zhang, S. B. Zhang, J. Liu, *J. Membr. Sci.* **2011**, *372*, 49–56.

24 D. S. Kim, Y. S. Kim, M. D. Guiver, B. S. Pivovar, *J. Membr. Sci.* **2008**, *321*,199–208.

25 C. S. Marvel, C. F. Bailey, M. S. Sparburg, *J. Am. Chem. Soc.* **1927**, *49*, 1833–1837.

26 L. Sheng, T. Higashihara, S. Nakazawa, M. Ueda, *Polym. Chem.* **2012**, *3*, 3289–3295.

27 L. Sheng, T. Higashihara, R. Maeda, T. Hayakawa, M. Ueda, *J. Polym. Sci., Part A: Polym. Chem.* **2013**, *51*, 2216–2224.

28 Y. S. Kim, D. S. Kim, B. Liu, M. D. Guiver, B. S. Pivovar, *J. Electrochem. Soc.* **2008**, *155*, B21–B26.

29 K. Hase, T. Nakano, A. Koiwai, *ECS Trans.* **2007**, *11*, 159–164.